Microsolvation Effect, Hydrogen-Bonding Pattern, and Electron Affinity of the Uracil−Water Complexes $U-(H_2O)_n$ ($n = 1, 2, 3$)

Xiaoguang Bao,[†] Huai Sun,[‡] Ning-Bew Wong,[§] and Jiande Gu*[,†]

Drug Design & Discovery Center, Shanghai Institute of Materia Medica, Shanghai Institutes for Biological Sciences, CAS, Shanghai 201203, P. R. China, College of Chemistry and Chemical Engineering, Shanghai Jiao Tong University, Shanghai 200240, P. R. China, Department of Biology and Chemistry, City University of Hong Kong, Kowloon, Hong Kong

Received: September 20, 2005; In Final Form: January 16, 2006

To achieve a systematic understanding of the influence of microsolvation on the electron accepting behaviors of nucleobases, the reliable theoretical method (B3LYP/DZP++) has been applied to a comprehensive conformational investigation on the uracil−water complexes $U-(H_2O)_n$ ($n = 1, 2, 3$) in both neutral and anionic forms. For the neutral complexes, the conformers of hydration on the O2 of uracil are energetically favored. However, hydration on the O4 atom of uracil is more stable for the radical anions. The electron structure analysis for the H-bonding patterns reveal that the $CH\cdots OH_2$ type H-bond exists only for di- and trihydrated uracil complexes in which a water dimer or trimer is involved. The electron density structure analysis and the atoms-in-molecules (AIM) analysis for $U-(H_2O)_n$ suggest a threshold value of the bond critical point (BCP) density to justify the $CH\cdots OH_2$ type H-bond; that is, $CH\cdots OH_2$ could be considered to be a H-bond only when its BCP density value is equal to or larger than 0.010 au. The positive adiabatic electron affinity (AEA) and vertical detachment energy (VDE) values for the uracil−water complexes suggest that these hydrated uracil anions are stable. Moreover, the average AEA and VDE of $U-(H_2O)_n$ increase as the number of the hydration waters increases.

Introduction

It is well-known that electron trapping on nucleic acid bases plays a crucial role in radiation-induced DNA damage since the acquisition of excess charge may start the cascade reactions that eventually lead to mutation and aging.[1−7] Recently, experimental and theoretical studies have demonstrated that, even at very low energies, electrons can induce strand breaks in DNA via dissociative electron attachment.[8−12] Moreover, the issue of the electron and hole transfer process in DNA and RNA also has attracted much attention.[13−26] Accurate electron affinities for DNA and RNA fragments and the distribution of excess electron sites are of great importance in understanding electron trapping related processes.[4,30,45] A number of experimental studies have been focused on the determination of the electron affinity (EA) of nucleic acid bases.[27−31]

Hydration of nucleic acid bases plays an important role in structural and biological processes. Many efforts have been devoted to investigating the interactions between water molecules and nucleic acid bases, and the base pairs as well.[32−42] In particular, hydration has been found to stabilize the radical anion of the nucleic acid bases,[30,43−45] turning the dipole-bound anion[4,46,47] into a valence-bound anion.[30,45] Sevilla et al.[43,44] rationalized and predicted the stabilizing effects of hydration on electron attachment to nucleic acid bases. Bowen and co-workers[45] investigated the one water molecule solvated uracil radical anion complex by photoelectron spectroscopy experiments. Their results showed that the transformation from a dipole-bound anion to a valence-bound anion took place when the radical anions experienced solvation and multibody interactions in the condensed phase. Schiedt and co-workers[30] studied the electron binding to the pyrimidine nucleobases in the presence of water clusters using photodetachment-photoelectron (PD-PE) spectroscopy. They found that the electron affinities were almost linearly proportional to the number of solvating water molecules.

Theoretical investigations of the electron attachment to nucleic acid bases at various levels of sophistication have complemented the experimental studies.[46,48−54] Theoretical EA determinations have been extended from single bases to base pairs[55−60] and from gas phase to microscopic solvated states.[61−65] The second-order Møller−Plesset perturbation theory (MP2) with a modest basis set including diffuse functions yields negative adiabatic electron affinity (AEA) values (ranging from −1.19 to −0.25 eV for the five bases),[50,51] while the density functional theory (DFT) approaches predict positive AEAs for both U and T.[50,54] Radical anions of the hydrogen-bonded uracil[66,67] and thymine dimer[68] were also theoretically studied. Both dipole-bound and valence-bound anions were predicted with the MP2 method.[66−68]

To understand the microsolvation effects, many efforts have been dedicated to investigations of uracil and uracil tautomers' interaction with water.[33,69−75] Preferential interaction sites of uracil with surrounding water molecules and the corresponding binding energies have been studied at different levels of theory.[33,71,73] The electrostatic potential features of hydrated uracil were examined by Gadre et al.[69] The influences of microsolvation on the tautomers of uracil were investigated with a DFT approach by Zeegers-Huyskens' group.[70] The protonation and deprotonation energies of uracil−water complexes were predicted at the MP4 and DFT levels of theory.[74] The effects

* To whom correspondence should be addressed. Phone: +86-21-50806720. E-mail: jiandegush@go.com.
[†] Shanghai Institutes for Biological Sciences.
[‡] Shanghai Jiao Tong University.
[§] City University of Hong Kong.

10.1021/jp055329r CCC: $33.50
Published on Web 03/02/2006

of hydration on the acidity of uracil were studied by Wetmore et al.[75] The influence of microhydration on the ionization of uracil and thymine were reported by Close et al.[42d]

Microscopic solvated models for a complex with uracil anions and one to three water molecules had been studied at the MP2 level of theory up to large basis sets (6-311++G(2df, 2p)).[61−64] Although the calculated vertical detachment energy (VDE) of the most stable anionic structure agreed with the experimental spectral maximum, the AEA seems to be underestimated by the MP2 approach.

However, an understanding of electron attachment to the solvated uracil is far from complete. Only limited conformers of the complexes of uracil with few water molecules have been explored.[61−64] The properties revealed in the earlier studies are mainly focused on the geometry and the electron affinity.[61−64] Important information such as the characteristics of the H-bonding pattern has been missing. In addition, the negative AEAs of uracil−water complexes predicted by the MP2 approach are inconsistent with the reliable experimental measurements.[30]

Recently, the development of a comprehensive DFT bracketing technique has provided a reliable method for electron affinity determination.[76] With this approach, the best estimation yields experimental-consistent AEA values and the relative AEA ordering of U > T > C ∼ G > A for individual bases.[54] With a reliably calibrated B3LYP/DZP++ approach, a more accurate bracketing of the electron affinities of 2′-deoxyribonucleosides has been accomplished.[77] Due to the influence of the 2′-deoxyribose, the AEAs of the studied species (dA, dG, dC, and dT) are all positive. The EAs of base pair GC[58] and AT[59] were predicted using DFT methods with DZP++ and TZ2P++ basis sets.

To a systematic understanding of the influence of the microsolvation on the electron accepting behaviors of the nucleic acid bases, we applied the reliable theoretical method (B3LYP/DZP++) to a comprehensive conformational investigation on the uracil−water complexes in both neutral and anionic forms. The number of solvating water molecules ranges from 1 to 3. To characterize the H-bonding patterns in the microsolvation process, the electron structure of the H-bonding between the hydration water and uracil has been analyzed along with atoms-in-molecules (AIM) theory. This combined approach provides deeper insight concerning the hydration motif of the nucleobases. Also, the electron affinities investigated in this study reveal the physical feature at the nascent stage of the formation of the radical anions of nucleobases in aqueous solutions.

Method of Calculation

The DFT bracketing technique,[54,58,76,77] in which five generalized gradient approximation (GGA) exchange-correlation density functionals were used, demonstrated that reliable middle range values of both geometry and electron affinity are produced by the B3LYP functional, which is a combination of exchange from Becke's 3-parameter HF/DFT hybrid exchange functional (B3)[78] with the dynamical correlation functional of Lee, Yang, and Parr (LYP).[79]

The double-ζ quality basis sets with polarization and diffuse functions (denoted as DZP++) were used in the present study. The DZP basis sets were constructed by augmenting the Huzinaga−Dunning[80,81] contracted Gaussian double-ζ functions with one set of *p*-type polarization functions for each H atom and one set of five *d*-type polarization functions for each C, N, and O atom [α_p(H) = 0.75, α_d(C) = 0.75, α_d(N) = 0.80, α_d(O) = 0.85]. To complete the DZP++ basis sets, one even-tempered diffuse *s* function was added to each H atom, while sets of even-tempered diffuse *s* and *p* functions were centered on each heavy atom. The even-tempered orbital exponents were determined according to the prescription of Lee and Schaefer:[82]

SCHEME 1: Atomic Numbering Scheme of Uracil

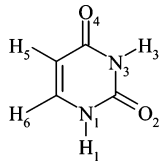

$$\alpha_{\text{diffuse}} = {}^1/_2\left(\frac{\alpha_1}{\alpha_2} + \frac{\alpha_2}{\alpha_3}\right)\alpha_1 \qquad (1)$$

where α_1, α_2, and α_3 are the three smallest Gaussian orbital exponents of the *s*- or *p*-type primitive functions for a given atom ($\alpha_1 < \alpha_2 < \alpha_3$). The final DZP++ set contains 6 functions per H atom (5s1p/3s1p) and 19 functions per C, N, or, O atom (10s6p1d/5s3p1d). This basis set has a significant tactical advantage, since it has been systematically examined in comprehensive calibrative studies[76] of a wide range of electron affinities. Also, previous studies illustrated that the DZP++ basis set is reliable for H-bonding structures.[58,59]

The geometries of the microsolvated uracil complexes U−$(H_2O)_n$ ($n = 1-3$) were fully optimized by analytic gradient techniques at the B3LYP/DZP++ level of theory. The analytical vibrational analysis was performed based on these optimized structures at the same level of theory. The Gaussian 98 package of programs[83] was used in the calculations.

To analyze the H-bonding patterns in the microsolvated uracil complexes, the AIM theory of Bader[84,85] was applied.

Results and Discussion

The atomic numbering scheme for the following discussion is based on Scheme 1.

1. Geometry and Relative Energy. *U−H₂O.* Four conformations of one-water hydrated uracil complex have been located as the local minima on the potential energy surface. The corresponding radical anions have also been optimized at the same level of theory (B3LYP/DZP++). The main geometric parameters of these optimized structures are summarized in Figure 1. The overall structures of the neutral species are found to be similar to those studied at the MP2 level of theory with various basis sets (up to 6-311++G(d,p)).[33,63,73]

The most significant alteration in the geometry of the radical anion is the dramatic elongation of the NH···OH_2 atomic distances. The NH···OH_2 atomic distance varies from 2.44 Å for U1-3a to 3.19 Å for U1-4a. As expected, due to the extra electron attachment on uracil, the proton donation of the N3 of uracil is greatly suppressed. On the other hand, the proton accepting ability is increased in the radical anions. The O···HOH bond lengths in the radical anion complexes are about 0.22 Å shorter than those in the corresponding neutral species. It should be noted that the differences of H-bond distances between the DFT values and the MP2 predictions are even more profound for the radical anions. The predicted O···HOH bond lengths are about 0.05−0.10 Å shorter at the B3LYP/DZP++ level of theory (as compared with the MP2 values).[63]

The relative energies of the computed species are summarized in Table 1. The most stable conformer of the neutral uracil−water complexes is U1-3. The relative stability sequence has been found to be U1-3 > U1-2 ∼ U1-4 > U1-1. The conformers

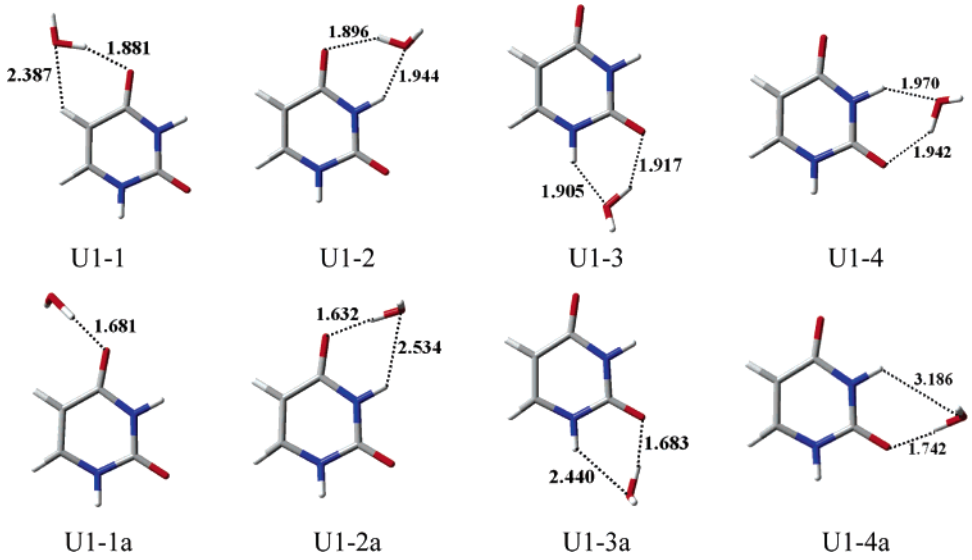

Figure 1. Optimized structure of U−H_2O (U1-*x*, *x* = 1, 2, 3, 4) and the corresponding radical anion (U1-*x*a, *x* = 1, 2, 3, 4). The colors represent the following atoms: gray is for carbon, white is for hydrogen, red is for oxygen, and blue is for nitrogen. The units of the bond length are angstroms.

TABLE 1: Relative Energy of the Monohydrated Uracil Complexes

	ΔE^a	$\Delta E_{ZPE}{}^b$		ΔE^a	$\Delta E_{ZPE}{}^b$
	Neutral			Anion	
U1-1	3.38	3.07	U1-1a	0.00	0.00
U1-2	1.62	1.54	U1-2a	0.09	0.31
U1-3	0.00	0.00	U1-3a	1.86	2.26
U1-4	2.30	2.14	U1-4a	2.96	3.05

[a] ΔE (in kcal/mol) is the relative energy. [b] ΔE_{ZPE} is the zero-point energy corrected relative energy.

in which the water molecule forms a hydrogen-bond with the O2 atom of uracil are more stable, which was the same with the previous studies.[33,71] However, this stability order reverses in the radical anions. Due to the electron attachment to uracil, the conformers with O4 H-bonding to water are more stable and the relative stability follows the order U1-1a ∼ U1-2a > U1-3a > U1-4a.

U−$(H_2O)_2$. There are rich conformational topologies when the uracil interacts with two water molecules. Nine different conformers of the complex were optimized as the local minima at the B3LYP/DZP++ level of theory. All of these neutral conformers are similar to those previously reported by van Mourik et al. at the MP2 level of theory[72] and by others[42c,71] at the DFT level of theory. On the basis of the geometry of these complexes, the radical anionic uracil−$(H_2O)_2$ clusters were optimized and resulted in nine local minima.

According to the geometric feature of the neutral species, these di-water solvated uracil complexes can be classified into three types (Figures 2−4). Type I contains complexes with two water molecules H-bonded to uracil at separate positions (U2-1, U2-2, and U2-3), type II consists of a species with two water molecules H-bonded to uracil at adjacent positions (U2-4 and U2-5), and type III are those with a water dimer H-bonded to uracil (U2-6, U2-7, U2-8, and U2-9).

Notice that the O4···HOH and the C5H···OH_2 atomic distances (1.88 Å for the former and 2.41 Å for the latter) in U2-1 are basically the same as those in U2-3 (1.87 Å and 2.40 Å, respectively); the H-bonding at this position seems unaffected by the position of the second hydration water. On the contrary, compared to U2-2, the O2···HOH bond length (1.93 Å) is 0.016 Å longer and the N1H···OH_2 bond distance (1.90 Å) is 0.01 Å shorter in U2-1. This geometric difference implies the important difference in H-bonding for the water at the O4−C5H position and at the O4−N3H position of the uracil, which might imply that the water has only one H-bond at the O4−C5H position while it has two H-bonds at the O4−N3H position of the uracil.

When water molecules interact with the uracil at the adjacent positions either O4 (in U2-4) or O2 (in U2-5) forms a bifurcated H-bond to the protons from water. The bifurcated O···HOH bond lengths are significantly longer than those of the normal H-bond (Figure 3).

For type III, the water dimer acts as one water molecule in U−H_2O complexes. However, the O···HOH and the NH···OH_2 bond lengths here are remarkably shorter than those in one-water solvated species (see Figure 4). Also, the C5H···OH_2 atomic distance in U2-6 amounts to 2.20 Å, about 0.19 Å shorter than that in U1-1. A water dimer seems to be a better H-bonding receptor and donator as compared to a single water molecule.

The attachment of an extra electron to uracil results in a significant decrease in the O···HOH bond lengths (typical bond length amounts to 1.54−1.68 Å, about 0.20 Å shorter than those in the neutral complexes) and a profound increase in the NH···OH_2 atomic distances, which are similar to those in U−H_2O complexes. The uracil anions are hydrated only on their O4 and O2 positions with the exception of U2-9a, in which the N1H···OH_2 atomic distance of 2.11 Å suggests a weak H-bond.

The most stable conformer of the neutral species of dihydrated uracil has been found to be U2-9, which is consistent with the results with van Mourik.[72] It is interesting to note that the hydration position of the water dimer in U2-9 is the same as that of the water in U1-3, which is the most stable one in the U−H_2O complexes. In general, the conformers with a water dimer are more stable than the others. Compared to single water molecule, a water dimer seems to have a stronger hydration ability (see Table 2). This is consistent with the previous conclusion by Mourik.[72]

For the radical anions, conformers with water molecules H-bonding to the O4 atom of uracil are energetically favored (U2-4a and U2-6a), which is also consistent with that found in the anionic U−H_2O complexes. It should be noted that although the energy of the neutral species U2-3, U2-4, and U2-6 is about 7 kcal/mol higher than that of the most stable one (U2-9), the

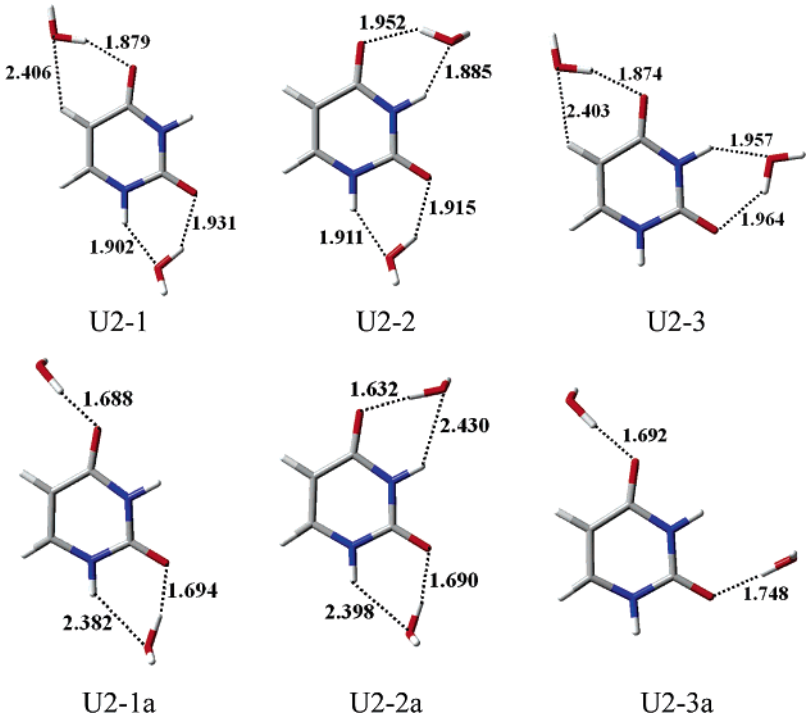

Figure 2. Optimized structure of $U-(H_2O)_2$ of type I and the corresponding radical anion. In this type, two water molecules H-bonded to uracil at separate positions. The colors represent the following atoms: gray is for carbon, white is for hydrogen, red is for oxygen, and blue is for nitrogen. The units of the bond length are angstroms.

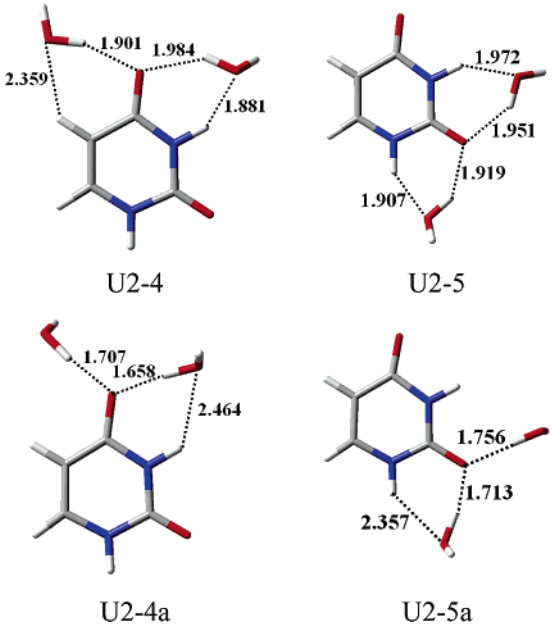

Figure 3. Optimized structure of $U-(H_2O)_2$ and the corresponding radical anion (type II). Two water molecules H-bonded to uracil at adjacent positions. The colors represent the following atoms: gray is for carbon, white is for hydrogen, red is for oxygen, and blue is for nitrogen. The units of the bond length are angstroms.

low energy of the corresponding radical anions (U2-3a, U2-4a, and U2-6a) suggests the importance of these conformers.

$U-(H_2O)_3$. Eleven conformers of neutral complexes and the corresponding radical anions consisting of one uracil and three water molecules were optimized as the local minima on the potential energy surface. Five of the neutral conformers (U3-2, U3-5, U3-7, U3-10, and U3-11) have been studied by Ghomi,[71] van Mourik,[72] and Hu.[42c] The geometric parameters of these neutral species are close to those reported in the literature (differences of the H-bond lengths are less than 0.04 Å).[42c,71,72] The three hydration water molecules are separated in U3-1, U3-9, and their corresponding anions. In U3-11 and U3-11a, they form a linearly H-bonded water trimer. A water dimer seems to be the most favorable since it is found in all other $U-(H_2O)_3$ complexes.

Similar to the uracil hydrated with two waters, the O···HOH and the NH···OH_2 bond lengths between water and uracil are short for the water dimer. However, due to the existence of the third hydration water, these H-bonds in the $U-(H_2O)_3$ complexes are slightly longer than those in the corresponding $U-(H_2O)_2$ complexes (see Figure 5). It is interesting to note that the C6H···OH_2 atomic distance in U3-11 amounts to 2.36 Å, about 0.04 Å shorter than the C5H···OH_2 atomic distance in U2-3 and U1-1.

For the radical anions of $U-(H_2O)_3$, the weak proton donating ability of uracil only exists in the complexes with a water dimer or trimer. This phenomenon is consistent with those observed in $U-(H_2O)_2$ and $U-H_2O$ radical anions. For U3-2a, three hydration waters are found to be closely H-bonded to O4 of the uracil anion with O···HOH bond distances of 1.678, 1.937, and 1.721 Å, respectively. Nevertheless, a similar hydration structure has not been detected for the O2 atom of uracil in our optimizations. The O4 atom is expected to be more negatively charged in the radical anion of uracil.

The most stable conformer of the neutral species of the trihydrated uracil is U3-7, and the next stable one is U3-8. Hydration on the N1−O2 moiety of uracil with a water dimer is the most stable form. The fact that U3-1 is 5.1 kcal/mol higher in energy than U3-7 suggests that the separated hydration pattern is less favored. Hydration with a water trimer seems also to be possible since the energy of U3-11 is only 1.84 kcal/mol higher than the most stable species (Table 3).

The extra negative charge on the uracil reverses the stability of the complexes. The separated hydration pattern (U3-1a) is energetically favored for the radical anions of $U-(H_2O)_3$. The even distribution of the negative charge on the separated

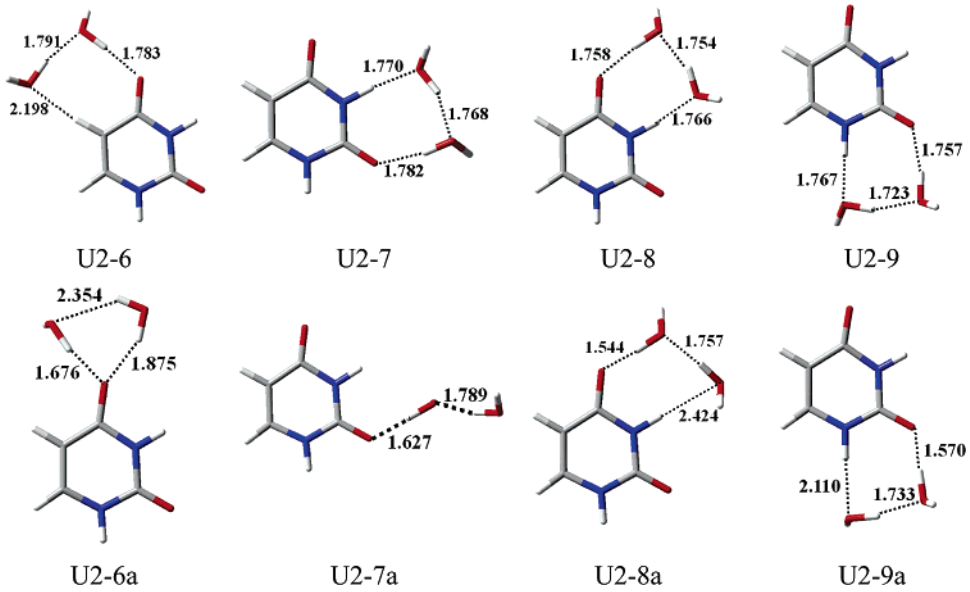

Figure 4. Optimized structure of U−$(H_2O)_2$ and the corresponding radical anion (type III). A water dimer is H-bonded to uracil in this type. The colors represent the following atoms: gray is for carbon, white is for hydrogen, red is for oxygen, and blue is for nitrogen. The units of the bond length are angstroms.

TABLE 2: Relative Energy of the Dihydrated Uracil Complexes

	ΔE^a	$\Delta E_{ZPE}{}^b$		ΔE^a	$\Delta E_{ZPE}{}^b$
	Neutral			Anion	
U2-1	5.44	4.69	U2-1a	1.04	1.08
U2-2	3.76	3.37	U2-2a	0.98	1.22
U2-3	7.64	6.28	U2-3a	2.33	2.06
U2-4	7.61	6.74	U2-4a	0.00	0.00
U2-5	4.61	4.06	U2-5a	4.71	4.83
U2-6	6.15	5.74	U2-6a	0.18	0.48
U2-7	3.46	3.17	U2-7a	5.60	5.56
U2-8	2.59	2.37	U2-8a	2.86	2.96
U2-9	0.00	0.00	U2-9a	4.17	4.79

[a] ΔE (in kcal/mol) is the relative energy. [b] ΔE_{ZPE} is the zero-point energy corrected relative energy.

hydration waters in U3-1a might be the physical background of the stability. The next most stable radical anion (U3-2a) is only 0.49 kcal/mol higher in energy. These low energy species suggest that hydration on the O4 atom of the uracil anion dominates the hydration pattern in the radical anions.

U3-11a, which is the least stable among the anions of U−$(H_2O)_3$, has been found to be 7.12 kcal/mol higher in energy than U3-1a. Notice that the water trimer structure still can be seen in U3-11a; the high energy of U3-11a implies that the water trimer structure is less important. The natural population analysis (NPA) charge indicates that the negative charge distribution on the water trimer in U3-11a is smaller than that in U3-1a (−0.08 vs −0.16).

2. H-Bonding Patterns. The density at the bond critical point (BCP) of the C5H···OH_2 interaction of U1-1 is found to be 0.009 au (see the Supporting Information). The C5H···OH_2 linkage might be a H-bond.[86,87] On the basis of the geometric feature, previous studies stressed the existence of this weak H-bond.[33,71] However, the electron density difference analysis performed at the present level of theory demonstrates that there is no electron density increase between the H5 of uracil and the O atom of water in the electron structure (Figure 6). Therefore, the interaction of C5H···OH_2 in U1-1 should not be classified as H-bonding.

Electron attachment to uracil greatly intensifies the proton accepting ability of uracil. Along with the significant reduction of the O···HOH bond distance (as short as 1.6−1.7 Å) of the uracil−water complexes, the corresponding density of the BCP remarkably increases up to 0.04−0.05 au in the radical anions. On the other hand, there is no proton donation from uracil observed for complexes U1-1a and U1-4a. The proton on N3 of U1-2a and N1 of U1-3a only weakly interacts with the O atom of water, signified by the long NH···OH_2 atomic distances of 2.53 Å for U1-2a and 2.44 Å for U1-3a. Accordingly, the corresponding density of the BCP is small (0.008 au for U1-2a and 0.009 au for U1-3a).

Consistently, the electron density difference maps displayed in Figure 7 demonstrate that there is no electron density increase between NH and OH_2.

It is important to note that, in the water-dimer hydrated complexes (U2-7, U2-8, and U2-9), not only are the BCP density values of the O···HOH bonds greatly increased (0.035−0.037 au), but the values of the NH···OH_2 bonds are also significantly intensified (0.039 au), signifying the improvement of the NH···OH_2 bonding. This BCP density increase implies that positive cooperative effects do exist for the H-bonding between uracil and the water dimer. As the result of the cooperative effects, relatively large BCP density is also detected for the C5H···OH_2 interaction in U2-6 (0.015 au). The distinct electron density increase between the C5H of uracil and the O of water confirms the H-bond (Figure 8).

Similar to the one-water hydrated uracil complexes, due to the extra electron attachment to uracil, the protons at the N1 and N3 atoms of uracil, in general, do not form H-bonds with the O of water in the radical anion complexes. However, there is one exception in which the proton at N1 of U2-9a seems to H-bond to O of hydration water. The relatively large density of the BCP at the N1H···OH_2 of U2-9a (0.018 au) and the distinguishable electron density increase between N1H of uracil and O of water in Figure 9 (U2-9a) support this conclusion.

The BCP density value at C5H···OH_2 in U3-2 and U3-3 amounts to 0.0158 and 0.0143 au, respectively, and that value at C6H···OH_2 in U3-11 amounts to 0.0107 au. The electron density deformation maps of C6H···OH_2 (of U3-11, Figure 10) and of C5H···OH_2 (of U3-2; see Figure 11) demonstrate a well-defined density increase between the proton and the oxygen of the hydration water. Therefore, the CH···OH_2 type of H-bond

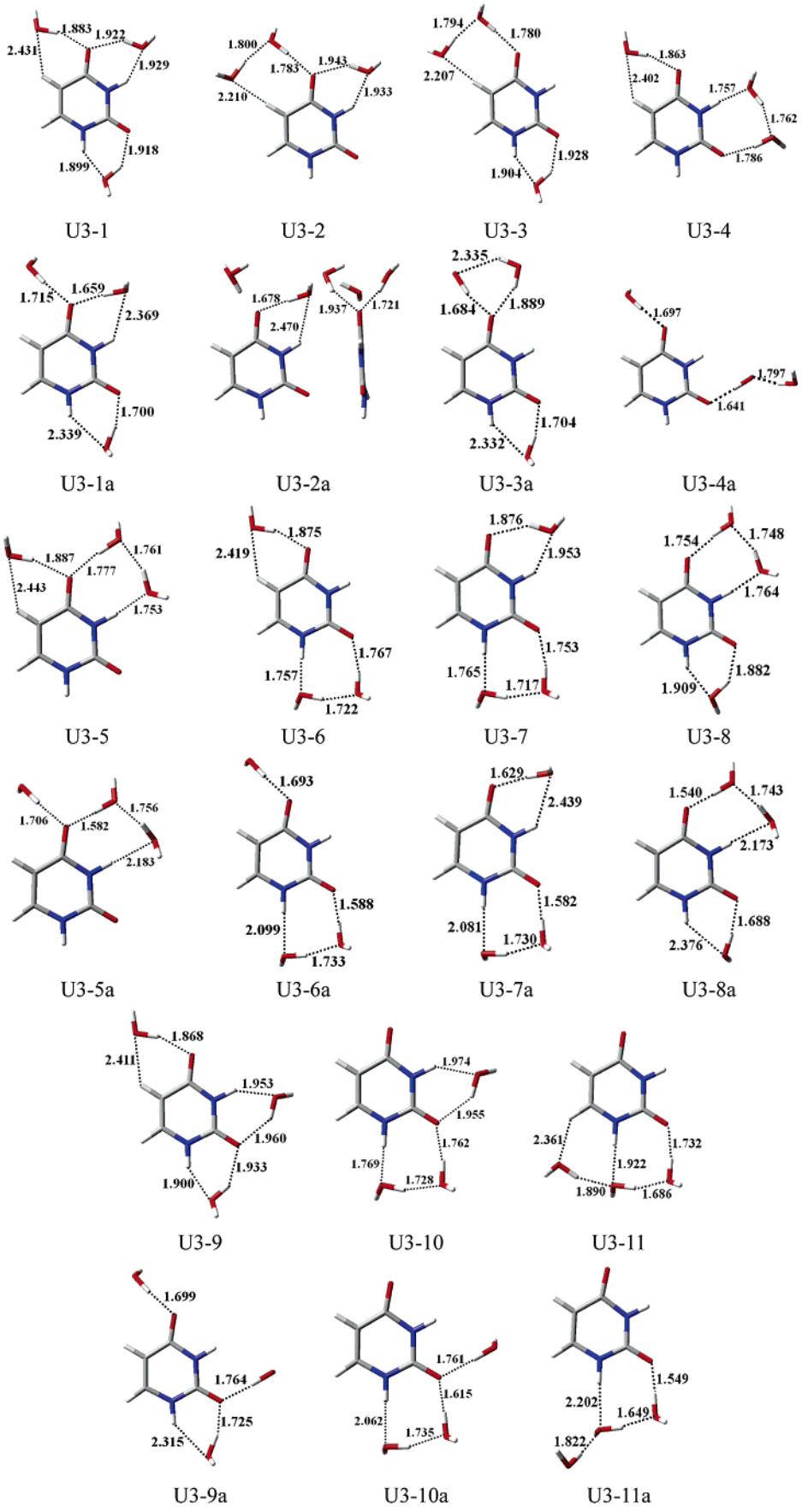

Figure 5. Optimized structure of $U-(H_2O)_3$ and the corresponding radical anion. U3 represents a complex of uracil with three water molecules. The colors represent the following atoms: gray is for carbon, white is for hydrogen, red is for oxygen, and blue is for nitrogen. The units of the bond length are angstroms.

TABLE 3: Relative Energy of the Trihydrated Uracil Complexes

	ΔE^a	$\Delta E_{ZPE}{}^b$		ΔE^a	$\Delta E_{ZPE}{}^b$
	Neutral			Anion	
U3-1	5.92	5.09	U3-1a	0.00	0.00
U3-2	7.00	6.52	U3-2a	0.32	0.49
U3-3	5.00	4.66	U3-3a	0.35	0.56
U3-4	5.20	4.70	U3-4a	4.10	3.63
U3-5	5.33	4.92	U3-5a	1.77	1.79
U3-6	2.14	1.84	U3-6a	2.11	2.35
U3-7	0.00	0.00	U3-7a	1.97	2.44
U3-8	1.00	0.95	U3-8a	2.50	2.69
U3-9	6.53	5.68	U3-9a	3.24	2.97
U3-10	1.67	1.55	U3-10a	6.12	6.44
U3-11	1.92	1.84	U3-11a	6.83	7.12

[a] ΔE (in kcal/mol) is the relative energy. [b] ΔE_{ZPE} is the zero-point energy corrected relative energy.

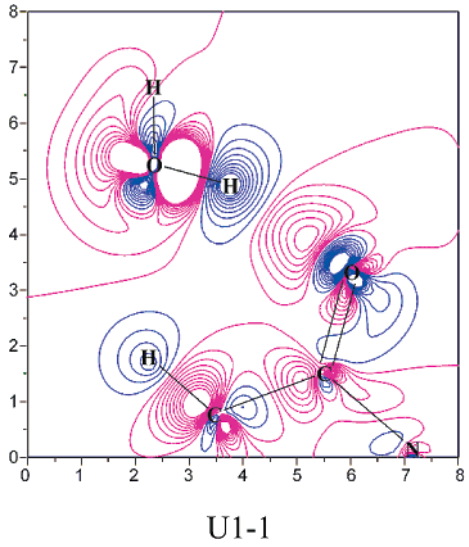

Figure 6. Electron density deformation map around the C5H···OH_2 moiety of U1-1. The term $\Delta\rho = \rho[U{-}H_2O] - \rho[U] - \rho[H_2O]$. Pink represents the density increase, and blue represents the density decrease. The contour line increase for pink is 0.0005 au, and for blue, it is −0.001 au. No electron density boost between C5H of uracil and O of water indicates that the C5H···OH_2 is not a H-bond.

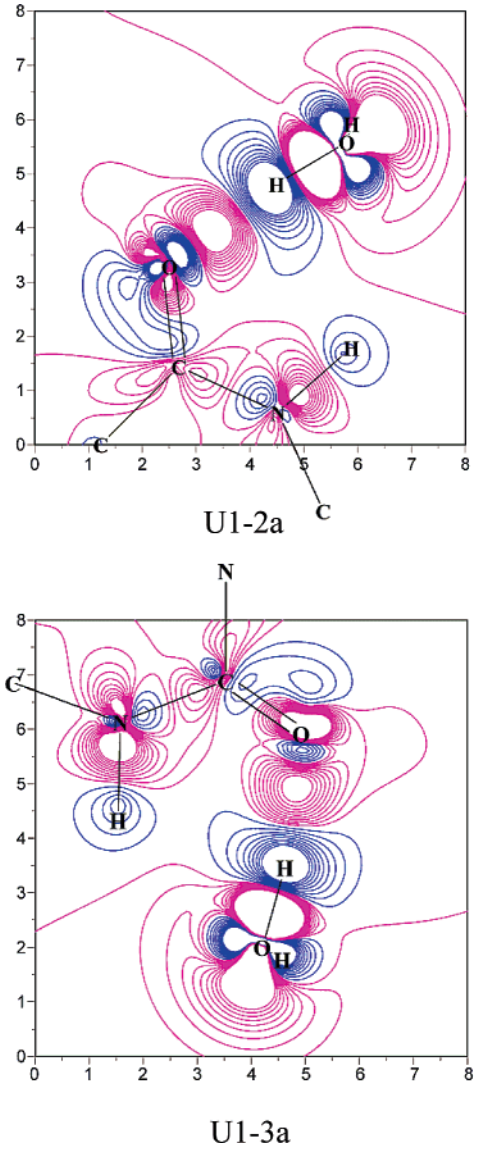

Figure 7. Electron density deformation map around the N3H···OH_2 moiety of U1-2a and U1-3a (N1H···OH_2 moiety). The term $\Delta\rho = \rho[(U{-}H_2O)^-] - \rho[U^-] - \rho[H_2O]$. Pink represents the density increase, and blue represents the density decrease. The contour line increase for pink is 0.0005 au, and for blue, it is −0.001 au.

is confirmed for these complexes. On the other hand, there is no density increase between the corresponding atoms in U3-1, U3-4, and U3-5, suggesting that the CH···OH_2 should not be assigned as a H-bond in these complexes.

Notice that the BCP densities of these non-H-bonding CH···OH_2 moieties are less than 0.010 au (0.0085 au for U3-1, 0.0087 au for U3-4, and 0.0086 au for U3-5); our electron density structure analyses for the U−$(H_2O)_n$ (n = 1, 2, 3) enable us to suggest a threshold value of the BCP density to justify the CH···OH_2 type of H-bond; that is, CH···OH_2 could be considered to be a H-bond only when its BCP density value is equal to or larger than 0.010 au.

3. Electron Affinities. Table 4 presents the B3LYP/DZP++ zero-point corrected AEAs, which were computed as the difference between the total energies of the appropriate neutral and anion species at their respective optimized geometries for the U−$(H_2O)_n$ (n = 1, 2, 3) complexes. All of the U−H_2O complexes have positive AEA values varied from 0.35 to 0.58 eV. U1-1 has the largest AEA value of 0.58 eV, and the average AEA value of these four complexes amounts to 0.46 eV, which is reasonably consistent with the PD-PE spectra determinations (the onset of the uracil−water complex is about 0.35 eV).[30,45] For comparison, the near-zero AEA values estimated by the MP2 methods[61,63] seem to be underestimated. Our theoretical AEA value suggests that microscopic solvation with one water molecule raises the AEA of uracil about 0.22 eV. The natural population analysis (NPA) shows that there is about 0.05 au of negative charge residing on the hydration water. The increased AEA might be partly attributed to this charge distribution. To explore the stability of the radical anion of the uracil−water complexes, the vertical detachment energies (VDEs) were calculated as the differences of the anionic UB3LYP energies and B3LYP energies of the corresponding neutral at the optimized anion geometries. The VDE of the four complexes ranges from 0.98 to 1.19 eV, and the average value is 1.10 eV, a relatively long lifetime is thus expected for these species.

The vertical attachment energies (VAEs) calculated as the energy differences of the neutral and the anion species at the optimized neutral geometries reveal that low energy is needed for the attachment of electrons during the nascent stage of the formation of the radical anions (lower than 0.16 eV, see Table 4). The radical anion of the uracil−water complexes could be easily formed through interaction with low energy electrons.

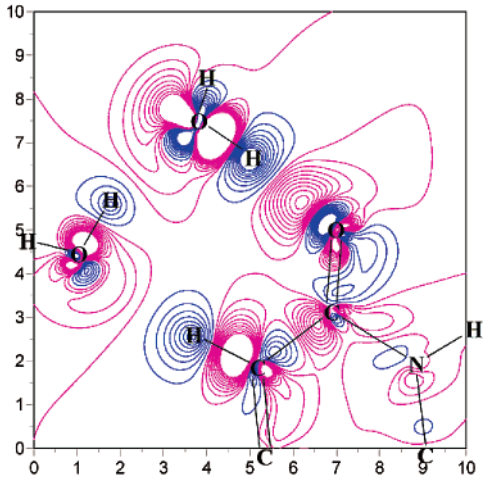

Figure 8. Electron density deformation map around the C5H···OH_2 moiety of U2-6. The term $\Delta\rho = \rho[U-(H_2O)_2] - \rho[U] - \rho[(H_2O)_2]$. Pink represents the density increase, and blue represents the density decrease. The contour line increase for pink is 0.0005 au, and for blue, it is −0.001 au. A well-defined density increase can be seen between C5H of uracil and O of water.

The AEA value of the dihydrated uracil complexes varies from 0.30 to 0.80 eV. The average AEA value of the nine calculated complexes amounts to 0.58 eV, about 0.12 eV higher than the corresponding value of monohydrated species. The NPA charge shows that there is about 0.10 au of negative charge residing on the water dimer in the radical anions. This charge distribution seems to stabilize the anions and therefore increase the AEA. The VDE of the dihydrated complexes ranges from 0.89 to 1.51 eV, which is consistent with the broad feature presented in anion PD-PE spectra.[30] The average VDE is 1.29 eV, about 0.19 eV larger than that of the one-water hydrated species. The vertical attachment energies calculated for the $U-(H_2O)_2$ species reveal that the energy needed during the nascent stage of the formation of radical anions is near-zero (the lowest VAE is −0.03 eV).

The AEA value of the trihydrated uracil complexes varies from 0.41 to 0.90 eV. The average AEA value of the eleven calculated complexes amounts to 0.67 eV, about 0.09 eV higher than the corresponding value of the dihydrated species. The VDE of the trihydrated complexes ranges from 1.11 to 1.71 eV with an average VDE value of 1.42 eV, about 0.13 eV larger than that of the dihydrated species. Similar to the dihydrated complexes, the vertical attachment energies calculated for the $U-(H_2O)_3$ species suggest that a low energy electron is ready to attach to trihydrated uracil (the lowest VAE is 0.01 eV).

The average AEA and VDE of $U-(H_2O)_n$ (n = 1, 2, 3) increase as the number of hydration waters increases, which is in agreement with the PD-PE experiments.[30] However, as compared to 0.22 eV for the average AEA increase per added water molecule,[30] the theoretical increase value is low (0.22 eV for n = 0 to n = 1; 0.12 eV for n = 1 to n = 2; and 0.09 eV for n = 2 to n = 3). The difference could be either due to the fact that conformers with different energy are averaged with the same weight or due to the uncertainty in using the onset of the structures of PD-PE spectra in the experimental determination.[30] It is interesting to note that the AEA increase rate of 0.23 eV is found for the most stable neutral conformers U2-9 to U3-7 and the increase rate of 0.22 eV is found for the most stable anion conformers U1-1a to U2-4a. An only 0.06 eV increase from U2-4a to U3-1a seems to suggest that there might

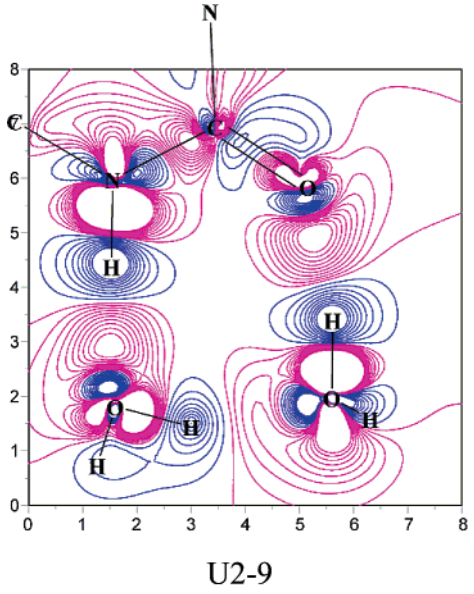

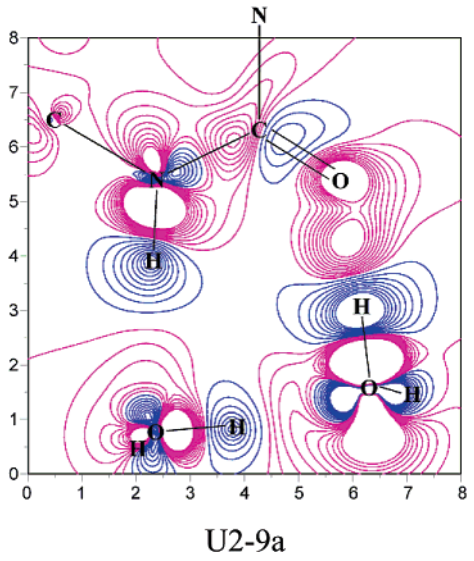

Figure 9. Electron density deformation map around the N1H···OH_2 moiety of U2-9 and U2-9a. For the neutral complex, $\Delta\rho = \rho[(U-(H_2O)_2)] - \rho[U] - \rho[(H_2O)_2]$, and for the anion complex, $\Delta\rho = \rho[(U-(H_2O)_2)^-] - \rho[U^-] - \rho[(H_2O)_2]$. Pink represents the density increase, and blue represents the density decrease. The contour line increase for pink is 0.0005 au, and for blue, it is −0.001 au.

be more stable radical anions existing for the trihydrated uracil complex. The search for these radicals is going on in our group.

Conclusions

The comprehensive and systematic investigation of the microsolvated uracil complexes $U-(H_2O)_n$ (n = 1, 2, 3) reveals that the water dimer is a better H-bonding receptor and donator when compared to the monomer or trimer in the hydration of uracil. Strong positive cooperative effects of the H-bonding between hydration water and uracil exist only when water molecules form a dimer. Cooperative effects do not exist for the H-bonding between uracil and the water monomer, although the uracil acts as both a proton donator and acceptor in these complexes.

For the neutral complexes, the conformers in which the water molecule forms a hydrogen bond with the O2 atom of uracil are favored in terms of energy. However, for the radical anions of uracil, hydration on the O4 atom of uracil is more stable.

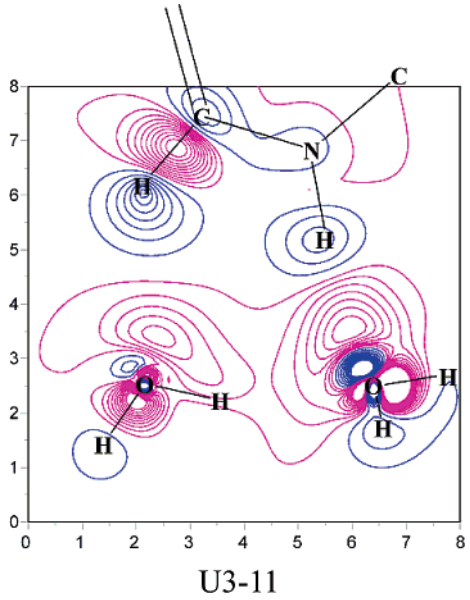

Figure 10. Electron density deformation map around the C6H···OH_2 moiety of U3-11. The term $\Delta\rho = \rho[U-(H_2O)_3] - \rho[U] - \rho[(H_2O)_3]$. Pink represents density increase, and blue represents the density decrease. The contour line increase for pink is 0.0005 au, and for blue, it is −0.001 au. The well-defined density boost along C6H···OH_2 indicates a H-bond.

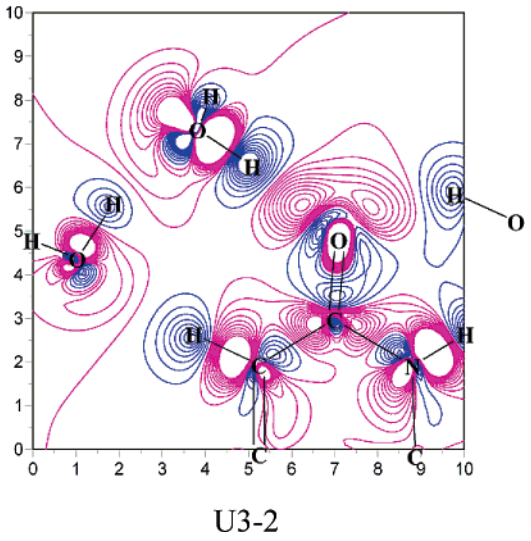

Figure 11. Electron density deformation map around the C5H···OH_2 moiety of U3-2. The term $\Delta\rho = \rho[U-(H_2O)_3] - \rho[U] - \rho[(H_2O)_3]$. Pink represents density increase, and blue represents the density decrease. The contour line increase for pink is 0.0005 au, and for blue, it is −0.001 au. The well-defined density boost along C5H···OH_2 indicates a H-bond.

The extra negative charge of the radical anion species of solvated uracil is mainly located on the uracil itself. This negative charge location greatly intensifies the proton accepting ability and, meanwhile, dramatically reduces the proton donating ability of uracil. Each solvating water molecule, therefore, interacts with anionic uracil through only one H-bond.

The electron structure analysis for the H-bonding patterns of U−$(H_2O)_n$ reveals that the CH···OH_2 type of H-bond exists only for di- and trihydrated uracil complexes in which a water dimer or trimer is involved. The interaction of C5H···OH_2 in monohydrated uracil should not be classified as H-bonding since there is no electron density increase between the H5 of uracil and the O atom of water in the electron structure.

TABLE 4: Electron Affinities of the Hydrated Uracil Complexes Using the B3LYP Functional With the DZP++ Basis Set[a]

	AEA[b]	VDE	VAE
	Uracil + $1H_2O$		
U1-1	0.58 (0.45)	1.19	−0.11
U1-2	0.50 (0.37)	1.12	−0.16
U1-3	0.35 (0.23)	0.98	−0.14
U1-4	0.41 (0.28)	1.09	−0.15
	Uracil + $2H_2O$		
U2-1	0.67 (0.54)	1.35	−0.03
U2-2	0.60 (0.47)	1.28	−0.12
U2-3	0.70 (0.58)	1.46	−0.07
U2-4	0.80 (0.68)	1.44	−0.05
U2-5	0.48 (0.34)	1.21	−0.14
U2-6	0.74 (0.61)	1.51	−0.03
U2-7	0.41 (0.25)	1.21	−0.26
U2-8	0.49 (0.34)	1.26	−0.20
U2-9	0.30 (0.17)	0.89	−0.12
	Uracil + $3H_2O$		
U3-1	0.86 (0.73)	1.58	0.00
U3-2	0.90 (0.77)	1.71	0.01
U3-3	0.82 (0.68)	1.66	−0.02
U3-4	0.68 (0.52)	1.56	−0.15
U3-5	0.77 (0.63)	1.52	−0.02
U3-6	0.62 (0.48)	1.28	−0.02
U3-7	0.53 (0.39)	1.20	−0.10
U3-8	0.56 (0.41)	1.34	−0.15
U3-9	0.76 (0.62)	1.56	−0.04
U3-10	0.43 (0.28)	1.11	−0.09
U3-11	0.41 (0.26)	1.12	−0.09
uracil	0.24 (0.12)[c]	0.76[d]	−0.14[d]

[a] The unit of the energy is electronvolts. [b] The AEA results are after zero-point energy correction, and in parentheses are uncorrected values. [c] Reference 54. [d] Present work.

The combination analysis of the electron density structure and the AIM for U−$(H_2O)_n$ (n = 1, 2, 3) suggests a threshold value of the BCP density to justify the CH···OH_2 type of H-bond; that is, CH···OH_2 could be considered as a H-bond only when its BCP density value is equal to or larger than 0.010 au.

Low energy electrons are easy to attach to the hydrated uracil because the vertical electron attachment energy is close to zero for U−$(H_2O)_n$ (n = 1, 2, 3). The positive AEA and VDE values for all the studied uracil−water complexes suggest that these hydrated uracil complexes form radical anions that are electronically stable. Moreover, the result that the average AEA and VDE of U−$(H_2O)_n$ increase as the number of the hydration waters increases clearly demonstrates that the radical anion of uracil could exist as an electronically stable species in aqueous solutions. Autodetachment of an electron is unlikely to happen.

Acknowledgment. This research project was supported by the "Knowledge Innovation Program", Chinese Academy of Sciences. The authors thank one of the referees for the suggestion to cite many references.

Supporting Information Available: Complete version of ref 83 and illustration of the BCPs of the uracil−water complexes. This material is available free of charge via the Internet at http://pubs.acs.org.

References and Notes

(1) Steenken, S.; Telo, J. P.; Novais, H. M.; Candeias, L. P. *J. Am. Chem. Soc*. **1992**, *114*, 4701−4709.

(2) Becker, D.; Sevilla, M. D. *Advances in Radiation Biology*; Academic Press: New York, 1993.

(3) Colson, A. O.; Sevilla, M. D. *Int. J. Radiat. Biol*. **1995**, *67*, 627−645.
(4) Desfrancois, C.; Abdoul-Carime, H.; Schermann, J. P. *J. Chem. Phys*. **1996**, *104*, 7792−7794.
(5) Kelley, S. O.; Barton, J. K. *Science* **1999**, *283*, 375−381.
(6) Ratner, M. *Nature* **1999**, *397*, 480−481.
(7) Huels, M. A.; Hahndorf, I.; Illengerger, E.; Sanche, L. *J. Chem. Phys*. **1998**, *108*, 1309−1312.
(8) Boudaiffa, B.; Cloutier, P.; Hunting, D.; Huels, M. A.; Sanche, L. *Science* **2000**, *287*, 1658−1659.
(9) Pan, X.; Cloutier, P.; Hunting, D.; Sanche, L. *Phys. Rev. Lett*. **2003**, *90*, 208102−208104.
(10) Caron, L. G.; Sanche, L. *Phys. Rev. Lett*. **2003**, *91*, 113201−113204.
(11) Berdys, J.; Anusiewicz, I.; Skurski, P.; Simons, J. *J. Am. Chem. Soc*. **2004**, *126*, 6441−6447.
(12) Barrios, R.; Skurski, P.; Simons, J. *J. Phys. Chem. B* **2002**, *106*, 7991−7994.
(13) Cai, Z.; Sevilla, M. D. *J. Phys. Chem. B* **2000**, *104*, 6942−6949.
(14) Messer, A.; Carpenter, K.; Forzley, K.; Buchanan, J.; Yang, S.; Razskazovskii, Y.; Cai, Z.; Sevilla, M. D. *J. Phys. Chem. B* **2000**, *104*, 1128−1136.
(15) Cai, Z.; Gu, Z.; Sevilla, M. D. *J. Phys. Chem. B* **2000**, *104*, 10406−10411.
(16) Lewis, F.; Letsinger, R.; Wasielewski, M. *Acc. Chem. Res.* **2001**, *34*, 159−170.
(17) O'Neill, M.; Becker, H.; Wan, C.; Barton, J.; Zewail, A. *Angew. Chem., Int. Ed*. **2003**, *42*, 5896−5900.
(18) Giese, B.; Spichty, M. *ChemPhysChem* **2000**, *1*, 195−198.
(19) Lewis, F.; Liu, J.; Zuo, X.; Hayes, R.; Wasielewski, M. *J. Am. Chem. Soc.* **2003**, *125*, 4850−4861.
(20) Jortner, J.; Bixon, M.; Langenbacher, T.; Michel-Beyerle, M. *Proc. Natl. Acad. Sci. U.S.A.* **1998**, *95*, 12759−12765.
(21) Henderson, P.; Jones, D.; Hampikian, G.; Kan, Y.; Schuste, G. *Proc. Natl. Acad. Sci. U.S.A.* **1999**, *96*, 8353−8358.
(22) Berlin, Y. A.; Burin, A. L.; Ratner, M. A. *J. Am. Chem. Soc*. **2001**, *123*, 260−268.
(23) Bixon, M.; Jortner, J. *J. Phys. Chem. A* **2001**, *105*, 10322−10328.
(24) Fink, H.; Schonenberger, C. *Nature* **1999**, *398*, 407−410.
(25) Robertson, N.; McGowan, C. *Chem. Soc. Rev*. **2003**, *32*, 96−103.
(26) Ratner, M. A.; Jortner, J. *Molecular Electronics*; Blackwell: Oxford, 1997.
(27) Ghen, E.; Chen, E.; Wentworth, W. *Biochem. Biophys. Res. Commun.* **1990**, *171*, 97−101.
(28) Wiley, J.; Robinson, J.; Ehdaie, S.; Chen, E.; Chen, E.; Wentworth, W. *Biochem. Biophys. Res. Commun.* **1991**, *180*, 841−845.
(29) Desfrancois, C.; Periquet, V.; Bouteiller, Y.; Schermann, J. *J. Phys. Chem. A* **1998**, *102*, 1274−1278.
(30) Schiedt, J.; Weinkauf, R.; Neumark, D.; Schlag, E. *Chem. Phys.* **1998**, *239*, 511−524.
(31) Periquet, V.; Moreau, A.; Carles, S.; Schermann, J.; Desfrancois, C. *J. Electron Spectrosc. Relat. Phenom.* **2000**, *106*, 141−151.
(32) Falk, M.; Hartman, K. A.; Lord, R. C. *J. Am. Chem. Soc*. **1962**, *84*, 3843−3846.
(33) van Mourik, T.; Price, S. L.; Clary, D. C. *J. Phys. Chem. A* **1999**, *103*, 1611−1618.
(34) Aleman, C. *Chem. Phys. Lett.* **1999**, *302*, 461−470.
(35) Aleman, C. *Chem. Phys.* **1999**, *244*, 151−162.
(36) Chandra, A. K.; Nguyen, M. T.; Uchimaru, T.; Zeegers-Huyskens, T. *J. Phys. Chem. A* **1999**, *103*, 8853−8860.
(37) Gu, J.; Leszczynski, J. *J. Phys. Chem. A* **1999**, *103*, 2744−2750.
(38) Moroni, F.; Famulari, A.; Raimondi, M. *J. Phys. Chem. A* **2001**, *105*, 1169−1174.
(39) Zhanpeisov, N. U.; Leszczynski, J. *J. Phys. Chem. A* **1998**, *102*, 6167−6172.
(40) Zhanpeisov, N. U.; Šponer, J.; Leszczynski, J. *J. Phys. Chem. A* **1998**, *102*, 10374−10379.
(41) Shishkin, O. V.; Gorb, L.; Leszczynski, J. *J. Phys. Chem. B* **2000**, *104*, 5357−5361.
(42) (a) Sukhanov, O. S.; Shishkin, O. V.; Gorb, L.; Podolyan, Y.; Leszczynski, J. *J. Phys. Chem. B* **2003**, *107*, 2846−2852. (b) Rejnek, J.; Hanus, M.; Kabeláč M.; Ryjáček, F.; Hobza, P. *Phys. Chem. Chem. Phys.* **2005**, *7*, 2006−2017. (c) Hu, X.; Li, H.; Liang, W.; Han, S. *J. Phys. Chem. B* **2004**, *108*, 12999−13007. (d) Close, D. M.; Crespo-Hernandez, C. E.; Gorb, L.; Leszczynski, J. *J. Phys. Chem. A* **2005**, *109*, 9279.
(43) Colson, A. O.; Besler, B.; Sevilla, M. D. *J. Phys. Chem.* **1993**, *97*, 13852−13859.
(44) Sevilla, M. D.; Besler, B. B.; Colson, A. O. *J. Phys. Chem.* **1994**, *98*, 2215.
(45) Hendricks, J. H,; Lyapustina, S. A.; de Clercq, H. L.; Bowen, K. H. *J. Chem. Phys.* **1998**, *108*, 8−11.
(46) Oyler, N.; Adamowicz, L. *J. Phys. Chem.* **1993**, *97*, 11122−11123.
(47) Hendricks, J. H.; Lyapustina, S. A.; deClercq, H. L.; Snodgrass, J. T.; Bowen, K. H. *J. Chem. Phys.* **1996**, *104*, 7788−7791.
(48) Sevilla, M.; Besler, B.; Colson, A. *J. Phys. Chem.* **1995**, *99*, 1060−1063.
(49) Li, X.; Cai, Z.; Sevilla, M. D. *J. Phys. Chem. A* **2002**, *106*, 1596−1603.
(50) Wetmore, S.; Boyd, R.; Eriksson, L. *Chem. Phys. Lett.* **2000**, *322*, 129−135.
(51) Russo, N.; Toscano, M.; Grand, A. *J. Comput. Chem.* **2000**, *21*, 1243−1250.
(52) Walch, S. *Chem. Phys. Lett.* **2003**, *374*, 496−500.
(53) Preuss, M.; Schmidt, W.; Seino, K.; Furthmuller, J.; Bechstedt, F. *J. Comput. Chem.* **2004**, *25*, 112−122.
(54) Wesolowski, S.; Leininger, M.; Pentchev, P.; Schaefer, H. *J. Am. Chem. Soc.* **2001**, *123*, 4023−4028.
(55) Al-Jihad, I.; Smets, J.; Adamowicz, L. *J. Phys. Chem. A* **2000**, *104*, 2994−2998.
(56) Smets, J.; Jalbout, A. F.; Adamowicz, L. *Chem. Phys. Lett.* **2001**, *342*, 342−346.
(57) Li, X.; Cai, Z.; Sevilla, M. *J. Phys. Chem. A* **2002**, *106*, 9345−9351.
(58) Richardson, N.; Wesolowski, S.; Schaefer, H. *J. Am. Chem. Soc*. **2002**, *124*, 10163−10170.
(59) Richardson, N.; Wesolowski, S.; Schaefer, H. *J. Phys. Chem. B* **2003**, *107*, 848−853.
(60) Kumar, A.; Knapp-Momammady, M.; Mishra, P. C.; Suhai, S. *J. Comput. Chem.* **2004**, *25*, 1047−1059.
(61) Smets, J.; McCarthy, W.; Adamowicz, L. *J. Phys. Chem.* **1996**, *100*, 14655−14660.
(62) Smets, J.; Smith, D. M. A.; Elkadi, Y.; Adamowicz, L. *J. Phys. Chem. A* **1997**, *101*, 9152−9156.
(63) Dologounitcheva, O.; Zakrzewski, V. G.; Ortiz, J. V. *J. Phys. Chem. A* **1999**, *103*, 7912−7917.
(64) Morgado, A.; Pichugin, K.; Adamowicz, L. *Phys. Chem. Chem. Phys.* **2004**, *6*, 2758−2762.
(65) Kumar, A.; Mishra, P. C.; Suhai, S. *J. Phys. Chem. A* **2005**, *109*, 3971−3979.
(66) Smith, D. M. A.; Smets, J.; Adamowicz, L. *J. Phys. Chem A* **1999**, *103*, 5784−5790.
(67) Hall, C. S.; Adamowicz, L. *J. Phys. Chem. A* **2002**, *106*, 6099−6101.
(68) Jalbout, A. F.; Smets, J.; Adamowicz, L. *Chem. Phys.* **2001**, *273*, 51−58.
(69) Gadre, S.; Babu, K.; Rendell, A. *J. Phys. Chem. A* **2000**, *104*, 8976−8982.
(70) Kryachko, E.; Nguyen, M.; Zeegers-Huyskens, T. *J. Phys. Chem. A* **2001**, *105*, 1934−1943.
(71) Gaigeot, M.; Ghomi, M. *J. Phys. Chem. B* **2001**, *105*, 5007−5017.
(72) van Mourik, T. *Phys. Chem. Chem. Phys.* **2001**, *3*, 2886−2892.
(73) van Mourik, T.; Benoit, D. M.; Price, S. L.; Clary, D. C. *Phys. Chem. Chem. Phys.* **2000**, *2*, 1281−1290.
(74) Nguyen, M. T.; Chandra, A. K.; Zeegers-Huyskens, Th. *J. Chem. Soc., Faraday Trans.* **1998**, *94*, 1277−1280.
(75) Di Laudo, M.; Whittleton, S. R.; Wetmore, S. D. *J. Phys. Chem. A* **2003**, *107*, 10406−10413.
(76) Rienstra-Kiracofe, J. C.; Tschumper, G. S.; Schaefer, H. F.; Nandi, S.; Ellison, G. B. *Chem. Rev.* **2002**, *102*, 231−282.
(77) Richardson, N.; Gu, J.; Wang, S.; Xie, Y.; Schaefer, H. *J. Am. Chem. Soc.* **2004**, *126*, 4404−4411.
(78) Becke, A. D. *J. Chem. Phys.* **1993**, *98*, 5648−5652.
(79) Lee, C.; Yang, W.; Parr, R. G. *Phys. Rev. B.* **1988**, *37*, 785−789.
(80) Huzinaga, S. *J. Chem. Phys*. **1965**, *42*, 1293−1302.
(81) Dunning, T. H. *J. Chem. Phys*. **1970**, *53*, 2823−2833.
(82) Lee, T. J.; Schaefer, H. F. *J. Chem. Phys*. **1985**, *83*, 1784−1794.
(83) Frisch, M. J.; et al. *Gaussian 98*, revision a.10; Gaussian, Inc.: Pittsburgh, PA, 2001.
(84) Bader, R. F. W. *Atoms in Molecules: a Quantum Theory*; Clarendon Press: Oxford, 1990.
(85) Bader, R. F. W. *Chem. Rev.* **1991**, *91*, 893−928.
(86) Koch, U.; Popelier, P. L. A. *J. Phys. Chem.* **1995**, *99*, 9747.
(87) Popelier, P. L. A. *J. Phys. Chem. A* **1998**, *102*, 1873−1878.